*Clays and Clay Minerals*, 1971, Vol. 19, pp. 137–150. Pergamon Press. Printed in Great Britain

# MIXED-LAYER KAOLINITE–MONTMORILLONITE FROM THE YUCATAN PENINSULA, MEXICO*

**L. G. SCHULTZ, A. O. SHEPARD, P. D. BLACKMON and H. C. STARKEY**
U.S. Geological Survey, Denver, Colorado 80225, U.S.A.

(*Received* 25 *September* 1970)

**Abstract**—Clay beds 1–2 m thick and interbedded with marine limestones probably of early Eocene age are composed of nearly pure mixed-layer kaolinite–montmorillonite. Particle size studies, electron micrographs, X-ray diffraction studies, chemical analyses, cation exchange experiments, DTA, and TGA indicate that clays from three different localities contain roughly equal proportions of randomly interlayered kaolinite and montmorillonite layers. The montmorillonite structural formulas average $K_{0.2}Na_{0.2}Ca_{0.2}Mg_{0.2}(Al_{2.5}Fe^{3+}_{1.0}Mg_{0.5})(Al_{0.75}Si_{7.25})O_{20}(OH)_{4}$, with a deficiency of structural (OH) in either the montmorillonite or kaolinite layers. Nonexchangeable $K^+$ indicates that a few layers are mica-like. Crystals are mostly round plates 1/10 to 1/20 $\mu$ across. The feature most diagnostic of the mixed-layer character is an X-ray reflection near 8 Å after heating at 300°C. The clays are inferred to have developed by weathering of volcanic ash and subsequent erosion and deposition in protected nearshore basins.

## INTRODUCTION

THE THREE clays described herein were part of a much larger suite of pottery clays collected from 1958 to 1964 by A. O. Shepard or obtained by her from Thompson (1958) in connection with their studies of contemporary Mayan potters of the Yucatan Peninsula. Most of the clays were kaolinite, montmorillonite, or attapulgite, but three were composed of material unlike any previously encountered by the authors. The three clays were tentatively interpreted from X-ray diffraction data as mixed-layer kaolinite–montmorillonite, and considerable additional analytical data obtained on purified material have confirmed this identification. Such a mixed-layer combination has been described previously only from Japan (Sudo, 1959; Sudo and Hayashi, 1956; Shimoyama, Johns and Sudo, 1969) and from Florida (Altschuler, Dwornik and Kramer, 1963). The exceptional purity of the Yucatecan material and the precision with which its chemical composition can therefore be characterized prompt this report.

In addition to studying the three original Yucatecan clay samples, two of the authors revisited the localities in October 1968 and collected 25 additional samples of the clay deposits and associated rocks for mineralogical and petrographic studies, primarily in the hope of determining the origin of the clay.

We are grateful for financial assistance from the Carnegie Institution of Washington which enabled two of the authors to revisit the three clay localities. We also are grateful for help from Jose Uc of Ticul, Daniel Coba of Becal, and Cecilia Cobb Cahun of Tepakan, which enabled us to locate or enter the clay mines.

## OCCURRENCE

### *Localities*

The Ticul clay deposit is located on the Hacienda Yocat, which is 5 km from the edge of Ticul on the road to Muna (Fig. 1). The deposit is reached by an inclined shaft whose portal is about 50 m northeast of the hacienda. Mining is by room and pillars. The mined area is about 50 × 100 m.

The Tepakan clay mines are on the southeast edge of the town about 100 m behind the house of Acoba Medina and are reached by vertical shafts. The shaft open in 1968 was 10 m deep. Clay is removed in all lateral directions from the bottom of the shaft until the opening is considered unsafe, when a new shaft is dug. Surrounding caved shafts indicated a mined area about 25 × 50 m.

The Becal clay deposit is 2–3 km southeast of the town, but the mines have not been worked for more than 10 yr and the clay was inaccessible in 1968. Only the limestone and soil at the surface were sampled. Becal clay described herein was obtained from R. H. Thompson.

The only surface outcrop of the mixed-layer kaolinite–montmorillonite that we saw was in the bottom of a sinkhole about 4 m deep located just east of Highway 269 and 3 km north of Tepakan.

*Publication authorized by the Director, U.S. Geological Survey.



https://doi.org/10.1346/CCMN.1971.0190302 Published online by Cambridge University Press

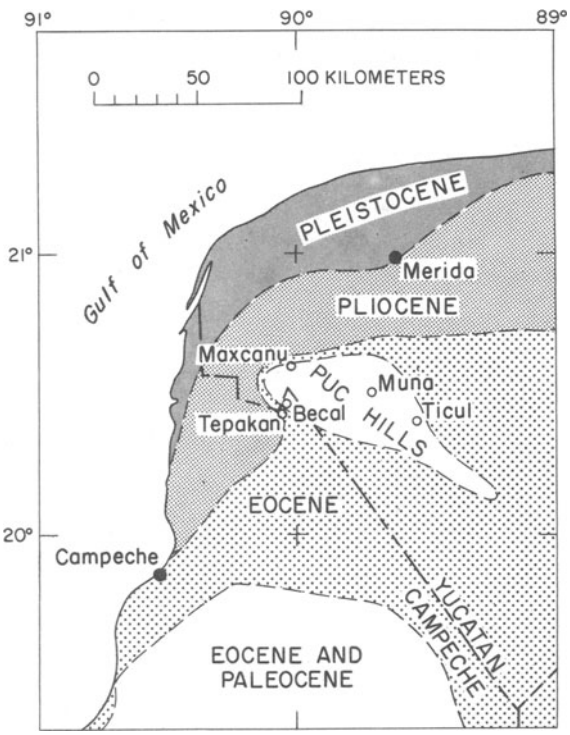



Fig. 1. Geologic map of the western part of the Yucatan Peninsula, adapted from Butterlin and Bonet (1963). Rocks of the Puc Hills are lower Eocene and Paleocene, undifferentiated.

*Geologic setting*

The clay beds are 1–2 m thick at all the observed localities. They are tabular and conformable with the enclosing limestones. The lower contact of the clay bed at Ticul is sharp, smooth, and slightly hummocky with a relief of a few cm. The lower contact at Tepakan was not seen, but an auger hole ended very abruptly on a hard surface that could not be penetrated with the auger and that was assumed to represent a sharp contact with underlying limestone. The upper contact at Ticul is sharp and the clay bed is separated from the overlying limestone by lenses of breccia 0–15 cm thick composed of fragments of clay and limestone. The clay bed at Tepakan grades upward into the overlying limestone through a mottled interval 2 m thick composed of brown clay and white limestone. At the sinkhole locality north of Tepakan the clay bed was poorly exposed, but the upper contact appeared to be similar to that at Tepakan; the lower contact was below water level. The main nonclay contaminant in the clay beds consists of angular, uncorroded fragments of limestone similar in appearance to the enclosing limestones. The clays are all slickensided and mottled brown with gray. The gray color tends to occur along slickensides. The brown coloring matter is goethite.

The three locations as plotted on Butterlin and Bonet's (1963) geologic map (Fig. 1, this rep.) indicate that the Ticul and Becal clay beds both occur near the top of a unit of marine carbonates of undifferentiated early Eocene and Paleocene age. The Tepakan deposit, however, appears to be stratigraphically higher. The map, however, is a highly generalized one. The Puc Hills anticline (Fig. 1) is very asymmetrical, so that the beds dip about 15° NE off the anticline at Ticul but were seen to be nearly flat-lying in the Tepakan–Becal area. As the clay beds in the Tepakan–Becal area are all about the same depth below a nearly level surface and the localities only a few km apart, our hurried observations indicate that all the clay beds could be of the same age, probably upper Eocene.

*Petrology*

Thin-section study of the clay reveals a mass of mostly randomly oriented clay flakes, in keeping with the lack of bedding in hand specimens. Only locally are thin zones of clay oriented, apparently parallel to the slickensides prominent in hand specimens. The apparently low birefringence of the clay (0·003–0·005), judged from blue to yellow interference colors with a gypsum plate, could simply be due to extremely small grain size of the material. Index of refraction of plates in oil is about 1·52. Rare larger shredded plates (Bi= 0·007) appear to be kaolinite. Quartz occurs as equant subangular grains about 0·05–0·1 mm across. Goethite occurs as specks sprinkled in brown parts of the clay and as disseminated dust. Limestone fragments are composed of very fine grained calcite similar to that in adjacent beds and most have sharp boundaries with the surrounding clay. A few appear to be smeared out with tiny calcite particles sprinkled in the clay, along slickensides. The limestone fragments are sparse in most of the thin sections, but they are extremely abundant at the top of the Tepakan clay bed.

The limestones above and below the clay beds are composed of very fine particles of calcite (0·01 mm av.) with some areas where calcite has recrystallized into larger interlocking crystals. In some thin sections marine foraminifera are recognized.

Mineralogy of samples from the upper, middle, and lower parts of the Ticul and Tepakan clay beds is identical to that of the samples from these localities described in the following sections-predominantly mixed-layer kaolinite–montmorillonite, with minor kaolinite, quartz, and goethite. The limestones are, of course, predominantly calcite–

https://doi.org/10.1346/CCMN.1971.0190302 Published online by Cambridge University Press

no dolomite was recognized. Insoluble residues in the four analyzed limestone fragments in the clay beds, in the one limestone sample taken just above the breccia zone above the clay bed at Ticul, and in a limy sample from the transition zone above the Tepakan clay bed all are composed predominantly of mixed-layer kaolinite–montmorillonite and minor kaolinite and quartz, and thus they are mineralogically very similar to the clay beds. The amount of residue in most such samples is 7–10 per cent, but in the Tepakan transition zone 38 per cent residue was measured. Insoluble residues from higher limestone samples and also from the single sample taken from below the Ticul clay bed are all montmorillonitic and the residue tends to be relatively small in amount, ½–5 per cent, though 11 per cent montmorillonitic residue was found in a sample of soft limestone 4 m above the Tepakan bed.

Five samples of modern Terra Rosa soils developed on limestones above the clay deposits consist predominantly of poorly crystallized kaolinite with abundant hematite and a little quartz.

*Inferred origin*

The following origin, though highly speculative, accounts for the relations described above. A volcanic ash fall in Eocene time seems the most likely precursor of the clay beds because: (1) volcanic ash or montmorillonite derived from it is the parent material of the mixed-layer kaolinite–montmorillonite in Florida and Japan; (2) many volcanic ashes and bentonites derived therefrom are very low in quartz, as are the Yucatecan clays; (3) much volcanic debris occurs in the Tertiary rocks in the Gulf of Mexico region; and, (4) because an ash fall is one of the few reasonable mechanisms for introducing nearly pure aluminosilicate material into a sedimentary sequence dominated by carbonate rocks. Alteration of the ash, probably by weathering under acidic conditions, produced montmorillonite with H–Al interlayers partly in the form of gibbsite-like layers. Poncelet and Brindley (1967) have shown that such material converts readily to kaolinite. The weathering probably did not take place at the marine site of deposition. Acidic conditions are unlikely in a marine environment, and if they did occur, they would corrode limestone fragments in, and limestone beds below the clay beds. Weathering more likely occurred in nearby land areas, and the weathered material was transported by streams so sluggish that they could carry little material coarser than the very fine grained mixed-layer clays. Some of the transported material was disseminated into the sea and mixed with large proportions of clastic carbonate material, but in other areas along the coast the clay-bearing stream waters must have emptied into basins almost completely cut off from the sea, possibly by an offshore bar. Occasional storm waves breaking over the bar may have carried in the fragments of partly consolidated limestone that are the principal contaminants of the clay beds.

Deposition of nearly pure clay terminated when the protecting rim of the basin was breached or when the basin filled. Abrupt breaching seems most likely for the Ticul deposit, with entry of much fragmentary limy sediment, some wave erosion of the clay bed, and mixing of fragments of the two rock types in a breccia overlying the uneroded clay. The gradational upper contact of the clay bed at Tepakan seems better explained by basin filling or a more gradual breaching of the basin and gradual increase in carbonate sediment until conditions returned to the ocean-bottom deposition of fine-grained carbonate sediments normal to the area. Still later, the weathering conditions in the hinterland that produced the mixed-layer kaolinite–montmorillonite clay changed to more normal montmorillonite-producing regime as indicated by the montmorillonitic insoluble residue in limestones more than a meter or so above the clay beds. Compaction after burial produced the slickensides and percolating ground water moving along the fractures dissolved goethite, producing the present mottled coloration of the clays.

## PROPERTIES OF PURIFIED CLAYS

*Particle size and shape, and mineral analysis*

Sixteen grams of the Ticul, Tepakan, and Becal clays were handpicked to exclude calcite and brown clay containing goethite and to retain only the light-greenish-gray material. The brown parts of the mottled clays, according to mineralogical and chemical analyses not shown, contain 4–5 per cent of goethite; otherwise they are identical with the light-greenish-gray parts. The goethite-free greenish-gray clay was disaggregated in water with an ultrasonic probe and separated into sized fractions by centrifugation (Table 1). An unusual aspect of the three clays is the extremely small particle size. Not only is most of the disaggregated material finer than ¼ $\mu$ effective spherical diameter, but electron micrographs (Fig. 2) of the ¼–1 $\mu$ and 1–10 $\mu$ fractions show that much of the mixed-layer kaolinite–montmorillonite found by X-ray analyses of these coarser fractions is in aggregates of particles of about the same grain size as in the $< \frac{1}{4}\,\mu$ fraction. Because of the fine particle size of the samples, our usual method of preparing oriented aggregates on porous tiles for X-ray study could not be used, as most of the $< \frac{1}{4}\mu$

https://doi.org/10.1346/CCMN.1971.0190302 Published online by Cambridge University Press

Table 1. Particle size and mineralogical composition of Yucatecan clays
[(1) Ticul; (2) Tepakan; (3) Becal; tr, trace; –, none]

| | $< \frac{1}{4}\,\mu$ | | | $\frac{1}{4}$–1 $\mu$ | | | 1–10 $\mu$ | | | $> 10\,\mu$ | | | | | |
|---|---|---|---|---|---|---|---|---|---|---|---|---|---|---|---|
| | (1) | (2) | (3) | (1) | (2) | (3) | (1) | (2) | (3) | (1) | (2) | (3) | | | |
| | As per cent of total sample | | | | | | | | | | | | | | |
| | 85·7 | 92·1 | 71·7 | 11·0 | 6·9 | 22·5 | 1·4 | 0·6 | 5·4 | 1·9 | 0·4 | 0·4 | | | |
| | Minerals estimated as per cent of size fraction | | | | | | | | | | | | Per cent of total sample | | |
| | | | | | | | | | | | | | (1) | (2) | (3) |
| Mixed-layer kaolinite–montmorillonite | 100 | 100 | 100 | 70 | 40 | 90 | 25 | 70 | 75 | — | — | 10 | 93·8 | 95·3 | 96·0 |
| Kaolinite | — | — | — | 25 | 50 | 5 | 10 | 5 | 10 | — | — | — | 2·9 | 3·5 | 1·7 |
| Mica | — | — | — | — | 5 | — | — | — | — | — | — | — | — | 0·3 | — |
| Quartz | — | — | — | — | tr | 5 | 60 | 20 | 10 | 90 | 100 | 90 | 2·6 | 0·6 | 2·0 |
| K-feldspar | — | — | — | — | — | — | tr | tr | tr | — | — | — | tr | tr | tr |
| Anatase | — | — | — | 5 | 5 | tr | 5 | 5 | 5 | — | — | — | 0·7 | 0·3 | 1·1 |
| Calcite | — | — | — | — | — | — | — | — | — | 10 | — | — | tr | — | — |

material went through the tile when a vacuum was applied under it. Glass slides, smears, or porous tiles without vacuum were used instead.

X-ray analyses show that mixed-layer kaolinite–montmorillonite comprises about 95 per cent of all three of the clay samples and is the only component detected in the $< \frac{1}{4}\,\mu$ fraction. Some of the kaolinite in the coarser fractions shows typical hexagonal crystal edges. Most quartz particles are moderately well rounded (Fig. 2). Crystals with square outlines in the micrographs of the Ticul 1–10 $\mu$ fraction and Tepakan $\frac{1}{4}$–1 $\mu$ fraction may be the anatase detected by X-ray in the coarser fractions of these samples.

Most of the mixed-layer kaolinite–montmorillonite crystals (Fig. 2, $< \frac{1}{4}\,\mu$ fractions) are nearly round and are 1/20–1/10 $\mu$ across. The particles must be flakes, as indicated by their high degree of preferred orientation when they are settled from a water suspension onto a glass slide. A few small crystals, indicated by the arrows on Fig. 2, have fairly good hexagonal outlines. It is not known if such hexagonal particles are mixed-layer kaolinite–montmorillonite or if they are kaolinite crystals that are too sparse to be detected in the X-ray analysis. If the particles are kaolinite crystals, they are too small a part of the $< \frac{1}{4}\,\mu$ fraction to affect the chemical analyses appreciably.

*X-ray diffraction*

X-ray diffractometer traces for the Ticul sample are shown in Fig. 3 and partial traces for the Tepakan and Becal samples are shown in Fig. 4. Patterns beyond 30° 2$\theta$ are virtually identical for all three clays.

The trace of the unoriented aggregate (Fig. 3) shows only broad, weak reflections. Those near 20°, 35°, 55°, and 62° 2$\theta$ correspond to the *hk* bands that, because of their similar, nearly orthohexagonal structures, are common to all lamellar silicates. Of these, only the 06 bands, which are single broad reflections centering at 1·494, 1·495, and 1·497 Å spacings for Ticul, Tepakan, and Becal clay, respectively, are normally useful for identification. These *d*-spacings are intermediate between those expected for dioctahedral kaolin minerals and three-layer mica-like or montmorillonite-like minerals.

All other reflections are considered, on the basis of their very considerable enhancement by orientation, to be basal reflections. Their behavior after several treatments commonly used for clay mineral identification seems, from the discussion that follows, to be compatible only with a mixed-layer interstratification of kaolin-like and montmorillonite-like layers.

The only other clay mineral that closely resembles the Yucatecan clays in some of its X-ray properties is slightly hydrated halloysite. Therefore, a listing of the features that distinguish mixed-layer kaolinite–montmorillonite from halloysite might be useful. The 06 *d*-spacings of 1·494–1·497 Å are distinctly high for a kaolin mineral like halloysite. Halloysite does not produce the pronounced 3·3 Å reflection after the kaolin layers are destroyed at 550°C. Halloysite normally cannot be oriented so perfectly as the Yucatecan clays, though some platy halloysites have been described (Brindley and Souza Santos, 1966). Finally, the *d*-spacing near 8 Å after 300°C heating could not be from halloysite. Such heat treatment should eliminate all adsorbed water, and the layer thickness of halloysite should decrease to about 7·2 Å. The 8·0–8·4 Å reflections observed

https://doi.org/10.1346/CCMN.1971.0190302 Published online by Cambridge University Press

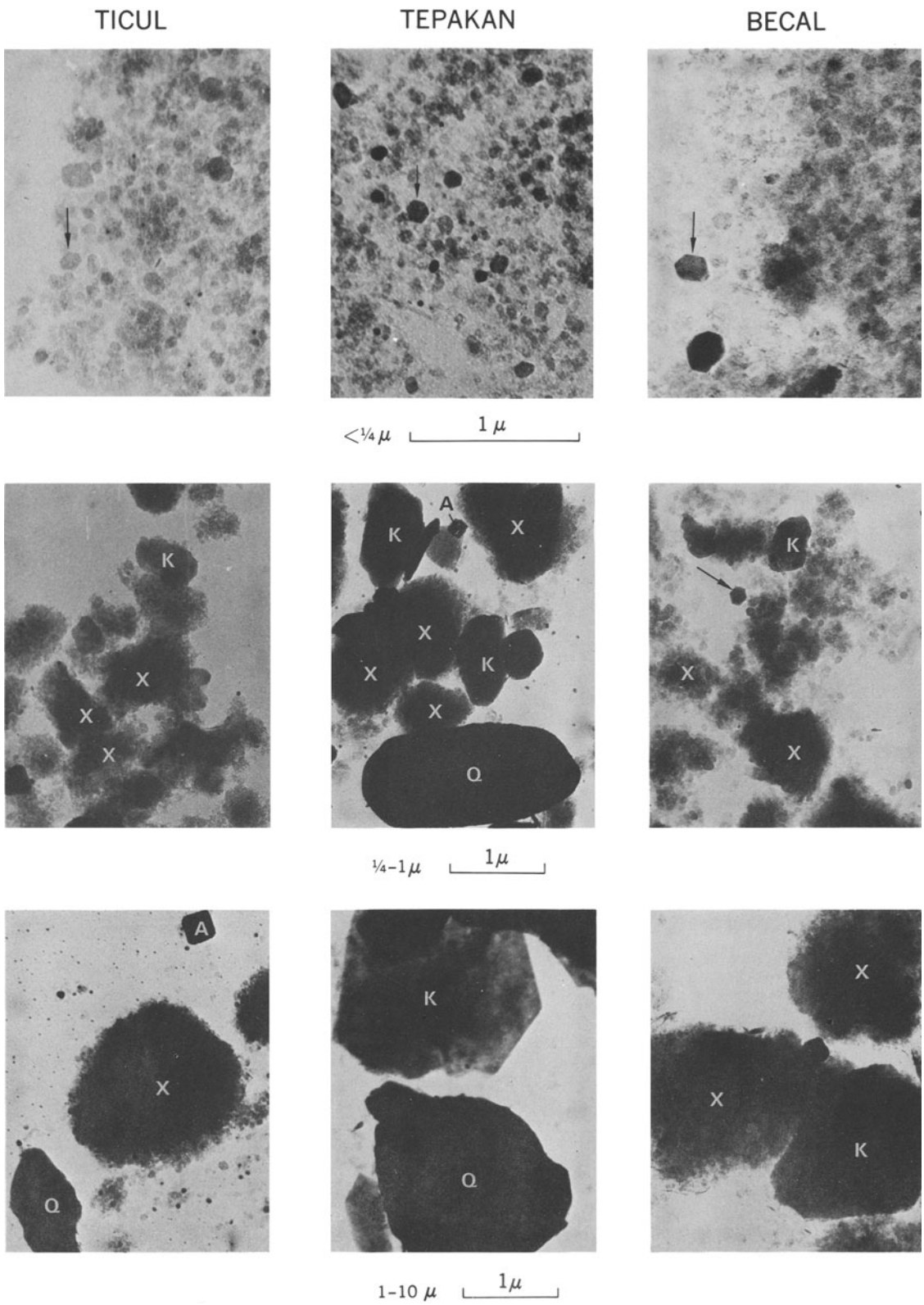



Fig. 2. Electron micrographs of size fractions. K – kaolinite, Q – quartz, A – anatase, X – aggregates of mixed-layer kaolinite–montmorillonite crystals. Arrows point to very small hexagonal flakes that may be kaolinite.

(*Facing page* 140)

https://doi.org/10.1346/CCMN.1971.0190302 Published online by Cambridge University Press

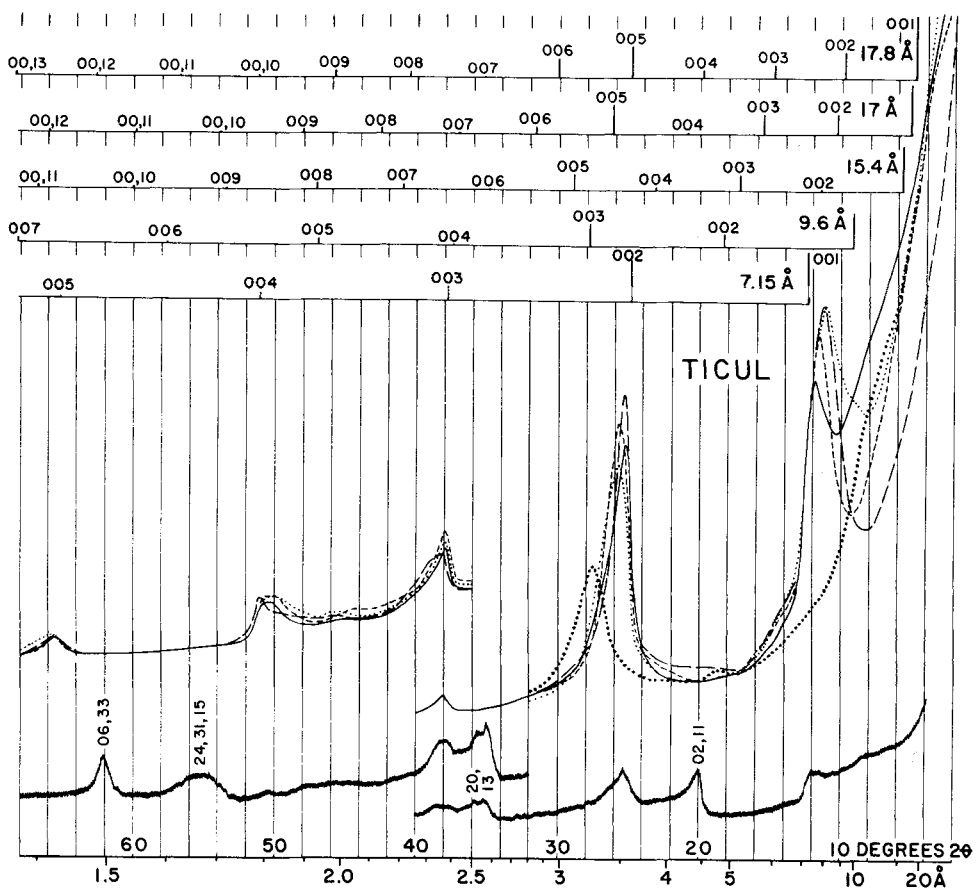



Fig. 3. X-ray diffractometer traces of $< \frac{1}{4}\mu$ Ticul clay. Unoriented powder, lower traces; oriented aggregates (smoothed traces) as follows, ——— air dried at 40 per cent r.h., – – – – ethylene glycol, ——— glycerol, ····· 300°C, ····· 550°C; 1° beam slit from 2° to 40° 2$\theta$, 4° beam slit from 36° to 68° 2$\theta$. Bar graphs at the top indicate positions and approximate intensities of basal orders for primary layer thicknesses given at the right. The *hk* indices above the trace of the unoriented powder are from Brindley (1961, p. 28 and 114) and MacEwan (1961, p. 192). Cu$K_\alpha$ radiation, sample length 40 mm.

after 300°C heating are the most easily observed and are the single most diagnostic feature of mixed-layer kaolinite–montmorillonite.

Mixed-layer crystals composed of layers of two different thicknesses produce basal X-ray reflections at *d*-spacings intermediate between the (00*l*) *d*-spacings of the two end-member layers. The exact position, shape, and intensities of the reflections depend upon the relative frequency and order of stacking of the different layers, differences in *d*-spacing, structure factors of the end-member layers, and the crystal size if the layers in each crystal are few (Ross, 1968). Regular alternation of layers gives a "superorder" basal reflection corresponding to the sum of the layer thicknesses and a series of higher-order reflections at rational repeat distances of the superorder. Irregular stacking of layers produces reflections at irrational repeat distances. Migration curves of peak positions with change in proportions of end-member layers generally follow an *S*-shaped curve. If the end-member *d*-spacings are far apart, the *S* is pronounced, if close together, the *S* is nearly a straight line. Reflections tend to be sharp and strong if the end-member reflections are close together and strong, and they are broad and weak if end-member reflections are far apart. If one end-member reflection is much stronger than the other, the weaker may have little effect on peak position. For detailed discussions of diffraction from mixed-layer crystals, see MacEwan *et al.* (1961) and Ruiz Amil *et al.* (1967).

Positions and approximate intensities of (00*l*) reflections for kaolinite and montmorillonite of

https://doi.org/10.1346/CCMN.1971.0190302 Published online by Cambridge University Press

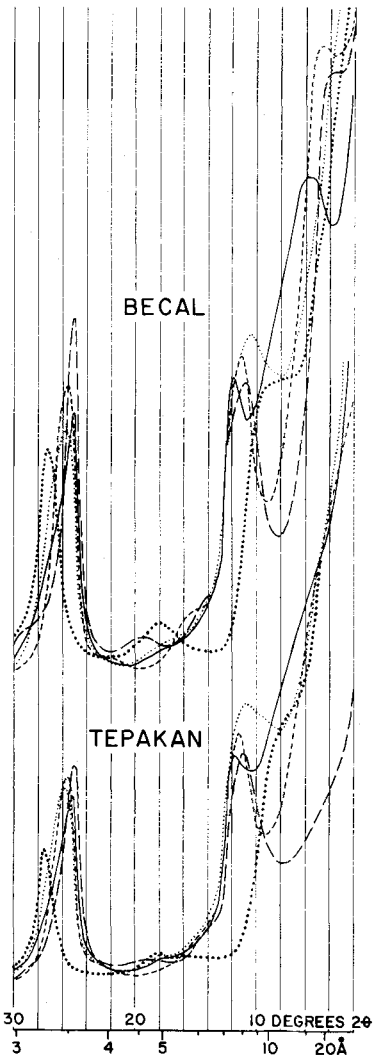



Fig. 4. X-ray diffractometer traces of oriented $< \frac{1}{4}\mu$ Becal and Tepakan clay. Symbols as on Fig. 3.

different layer thicknesses are shown at the top of Fig. 3: 17·8 Å for glycerol- and 17·0 Å for ethylene-glycol-saturated montmorillonite, 15·4 Å for air-dried montmorillonite with two layers of water, 9·6 Å for dehydrated montmorillonite, and 7·15 Å for kaolinite. Notation used for basal reflections in the following discussion is as follows: $17_{(001)}$, $17_{(002)}$, etc. or $9{\cdot}6_{(001)}$, $9{\cdot}6_{(002)}$, etc. for first, second, etc. orders of montmorillonite with these layer thicknesses; $M_{(00l)}$ for the montmorillonite basal reflections in general; $K_{(001)}$, $K_{(002)}$, etc. for kaolinite basal orders with an unvarying 7·15 Å layer thickness, and $K_{(001)}/17_{(002)}$ or $K_{(002)}/15{\cdot}4_{(005)}$ for reflections from mixed-layer combinations.

Positions for the basal reflections of the Ticul clay in Fig. 3 may be compared with those of $K_{(00l)}$ and $M_{(00l)}$ at the top of Fig. 3. Positions observed for the two strongest reflections are compared again on Fig. 5. The 7·45 Å reflection from material air-dried at about 40 per cent r.h. apparently is a $K_{(001)}/15{\cdot}4_{(002)}$ reflection intermediate between the 7·15 Å $K_{(001)}$ and the 7·7 Å $15{\cdot}4_{(002)}$ of montmorillonite. A predominance of double hydrate layers of montmorillonite with 15·4 Å thickness seems indicated for three reasons: (1) the $K_{(001)}/15{\cdot}4_{(002)}$ and $K_{(002)}/15{\cdot}4_{(005)}$ reflections resemble those of the Ca-saturated clay much more than they resemble those of the Na-saturated clay (Fig. 6) and, at the prevailing humidity, Ca-montmorillonite normally has a 15·4 Å layer thickness and two water layers rather than a 12·5 Å layer thickness and a single water layer (Mooney *et al.*, 1952, or see MacEwan, 1961, p. 171); (2) the layer thickness must be more than 14·9 Å to account for the observed 7·45 Å spacing; and, (3) layer thickness much above 15·4 Å are not likely at a r.h. below 50 per cent. Increases in $M_{(002)}$ to 8·5 Å after glycol saturation and to 8·9 Å after glycerol saturation account for the observed increases of $K_{(001)}/17_{(002)}$ to 7·7 Å and $K_{(001)}/17{\cdot}8_{(002)}$ to 7·9 Å. After 300°C heating, it is not $M_{(002)}$ but $M_{(001)}$ at about 9·6 Å that causes the final increase in the *d*-spacing to 8·0 Å. After 550°C

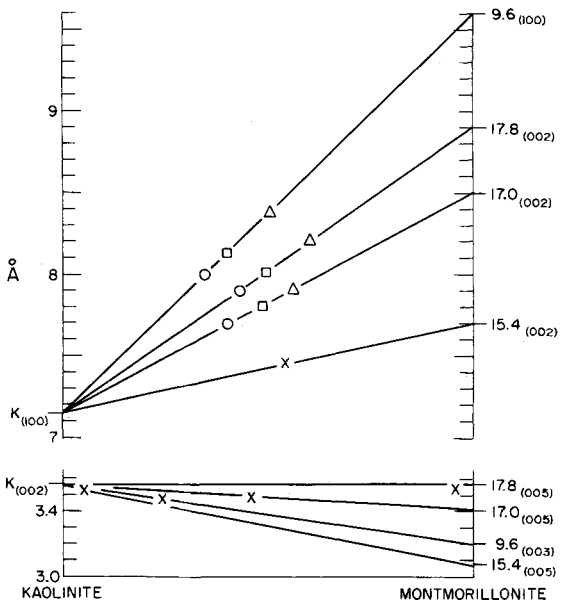



Fig. 5. Observed *d*-spacings of strongest $K_{(00l)}/M_{(00l)}$ reflections relative to *d*-spacings of unmixed end-members. Straight-line relations shown are close to calculated 7·14/10 migration curves of Brown and MacEwan (1951, p. 277, curves F). Ticul – ○; Tepakan – □; Becal – △; all samples – X.

https://doi.org/10.1346/CCMN.1971.0190302 Published online by Cambridge University Press

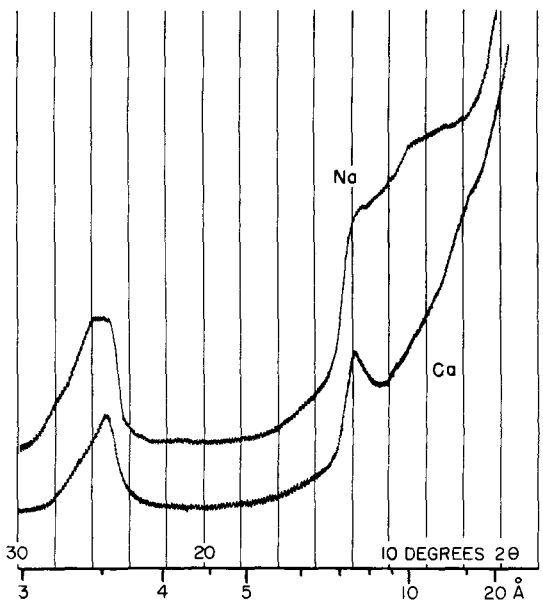



Fig. 6. X-ray diffractometer traces of Na- and Ca-saturated $< \frac{1}{4}\mu$ Ticul clay. 40 per cent r.h., Cu$K_\alpha$. K-, Li-, and H- saturated clays resemble Na; Mg-saturated resembles Ca.

heating, breakdown of kaolinite layers causes the reflection nearly to disappear. The remaining montmorillonite layers produce a pronounced $9{\cdot}6_{(003)}$ and a weak $9{\cdot}6_{(002)}$ and $9{\cdot}6_{(001)}$. The latter reflection may also result partly from the structural debris of the destroyed kaolin layers, which commonly gives a very broad reflection centering near 10 or 11 Å.

Most features of the basal reflections of the Tepakan and Becal clays (Fig. 4) are similar to those of the Ticul sample (Fig. 3). However, the air-dried $K_{(001)}/15{\cdot}4_{(002)}$ and the $K_{(001)}/9{\cdot}6_{(001)}$ are notably broader for Tepakan clay than for the other clays. The Becal clay differs mainly in the pronounced broad additional reflections centering near 16 Å, 20 Å, and 21 Å for air-dried, ethylene glycol-, and glycerol-saturated clay. These low-angle reflections seem not to be superorders of a regularly mixed-layer kaolinite–montmorillonite because (1) the *d*-spacings are not the sum of the layer thicknesses (e.g. glycol, 7 Å + 17 Å ≠ 20 Å), (2) they disappear after 300°C heating, and (3) their sequences of basal orders are irrational. Although the observed *d*-spacings are distinctly high for a separate montmorillonite phase, they are very broad. When the profiles of such broad reflections are corrected for Lorentz and polarization factors (Klug and Alexander, 1954, p. 683) which increase intensity of scattered radiation greatest at low $2\theta$ angles, the midpoints of the corrected reflections decrease for ethylene glycol and glycerol treated samples to near 17 Å and 18 Å spacings typical of montmorillonite. Yet, after 300°C heating, there is no sequence of basal orders from about 9·6 Å as should be produced by unmixed montmorillonite crystals. The best interpretation of the reflections observed in the 16–21 Å range seems to be as "isolated peaks" (MacEwan *et al.*, 1961, p. 417) which may appear when layer-thickness differences are very large and the normal intensity of one of the layers is very great; such reflections undergo only slight change of position and merely get stronger as the corresponding component increases in amount. The inferred higher proportion of montmorillonite layers in the Becal sample is in accord with several other features: (1) very broad and weak reflections near expected montmorillonite positions that are most pronounced for the Becal clay (note the 14°–22° $2\theta$ regions of Figs. 3 and 4); (2) the more pronounced 3·3 Å $M_{(003)}$ near 27° $2\theta$ after the kaolin layers of the Becal clay are destroyed by 550°C heating; (3) the previously mentioned 06 *d*-spacings, of which that for the Becal clay is largest and nearest that normal for montmorillonite; and (4), as will be seen, most chemical as well as other X-ray data. One exception is the $K_{(001)}/15{\cdot}4_{(002)}$ *d*-spacings (Fig. 5) which are identical for all three clays insofar as it can be measured. However, the 7·15 Å and 7·7 Å *d*-spacings that produce this reflection are too close together for a very accurate evaluation from such broad reflections. Other combinations with $K_{(001)}$ (Fig. 5) consistently indicate that the most montmorillonite occurs in the Becal sample. More kaolinite layers seem to be indicated in all three samples after the 300°C treatment than after the other treatments, but the relatively large *d*-spacing difference between $K_{(001)}$ and $9{\cdot}6_{(001)}$ makes the straight-line relations illustrated on Fig. 5 least likely for this combination.

The $K_{(002)}/M_{(00l)}$ reflections (Fig. 5) do not show quantitatively significant differences in *d*-spacings between samples, and only the $K_{(002)}/17_{(005)}$ peak positions indicate layer proportions that are approximately similar to those for the $K_{(001)}/M_{(00l)}$ reflections. Qualitatively, though, the reflections seem to make sense. The $K_{(002)}/17{\cdot}8_{(005)}$ reflections are all in similar positions and are relatively sharp and intense (Figs. 3 and 4) owing to the near coincidence of the two *d*-spacings. The $K_{(002)}/9{\cdot}6_{(003)}$ reflections are relatively broad and at slightly smaller *d*-spacings than with glycol or glycerol because the spacings are farther apart; the limited peak shift from the $K_{(002)}$ position probably indicates a strong *S*-shape to the layer-frequency vs. peak-position curve. The $K_{(002)}/15{\cdot}4_{(005)}$ reflection

https://doi.org/10.1346/CCMN.1971.0190302 Published online by Cambridge University Press

shifts even less from the $K_{(002)}$ position, probably because $K_{(002)}$ is closer to $15{\cdot}4_{(004)}$ than $15{\cdot}4_{(005)}$; the slight shift and marked asymmetry toward $15{\cdot}4_{(005)}$ probably reflect the much greater intensity of this reflection than the $15{\cdot}4_{(004)}$.

Similarity of the $K_{(003)}/9{\cdot}6_{(004)}$ and $K_{(003)}/17_{(008)}$ reflections is due to the near coincidence of all the *d*-spacings involved. The $17{\cdot}8_{(007)}$ and $17{\cdot}8_{(008)}$ of the glycerol treated material are nearly equidistant from $K_{(003)}$; the pronounced asymmetry toward the $17{\cdot}8_{(008)}$ reflection is due to its greater intensity relative to the $17{\cdot}8_{(007)}$. The discrepancy in this series of reflections is the symmetrical shape of the peak from air-dried material that, as with the reflection for glycerol treated clay, should be more asymmetrical toward $15{\cdot}4_{(007)}$.

The $K_{(004)}/17{\cdot}8_{(00,10)}$ is fairly sharp, owing to near coincidence of these *d*-spacings. Reflections of glycol-treated, air-dried, and 300°C-heated material are slightly shifted from $K_{(004)}$, and are strongly asymmetrical toward relatively intense $17_{(009)}$, $15{\cdot}4_{(008)}$, and $9{\cdot}6_{(005)}$ reflections although the nearly identical positions and intensities of $9{\cdot}6_{(005)}$ and $15{\cdot}4_{(008)}$ are not in accord with the relative weakness of the $K_{(004)}/15{\cdot}4_{(008)}$ reflection.

The reflections in the $K_{(005)}/M_{(00l)}$ group show little variation after the different treatments. The one consistent difference is the relatively great asymmetry toward $9{\cdot}6_{(007)}$ which is fairly far from $K_{(005)}$ and does not have a nearby and counterbalancing $9{\cdot}6_{(006)}$ as is the case for $17{\cdot}8_{(00,13)}$ and $17{\cdot}8_{(00,12)}$.

Observed X-ray diffractometer traces appear, at least qualitatively, to be in close accord with those theoretically expected from mixed-layer kaolinite–montmorillonite. Considering undetermined effects of (1) very fine particle size, (2) large differences in structure factors of kaolinite and montmorillonite layers, (3) deviation of layer-frequency vs. peak-position from assumed straight-line relations, (4) the unknown expanding characteristics of interlayer regions between kaolinite and montmorillonite layers, and (5) as will be demonstrated, the inclusion in the mixed-layer sequences of a small proportion of mica-like layers, the general agreement between observed X-ray scattering and that expected from a model so simple as an interlayering of expandable montmorillonite layers and nonexpandable kaolinite layers is remarkable. Discrepancies with theory are most common for the air-dried samples, suggesting deviation of some of the montmorillonite layers from the assumed 15·4 Å layer thickness. The X-ray analyses alone seem clearly to indicate that the clays must be randomly mixed-layer combinations predominantly of kaolinite–montmorillonite and that the Ticul sample contains a higher proportion of kaolin layers than do the other samples, and the Becal sample contains a higher proportion of montmorillonite layers. The exact proportion of layers cannot be determined by us from the X-ray data, but relations illustrated in Fig. 5 suggest that all of the samples have roughly equal proportions of the two layers.

X-ray analyses after various other chemical and heat treatments give some indication of the probable properties of the montmorillonite layers of the Yucatecan clays. When the layers are Mg saturated and treated with glycerol, the peak positions are similar to those shown on Figs. 3 and 4 for glycerol without Mg saturation, indicating that the montmorillonite layers still expand to about 17·8 Å. Therefore, the layers do not have a layer charge as high as that of vermiculite which should expand only to about 14·5 Å (G. F. Walker, in Brown, 1961, p. 315), the $14{\cdot}5_{(002)}$ of which (7·25 Å) in combination with the 7·15 Å $K_{(001)}$ could not account for the observed 7·45 Å reflections. However, expansibility with ethylene glycol is somewhat less when the clays are first K saturated and then heated to 300°C than it is without this treatment, indicating the layer charge is relatively high within the range common for montmorillonite (Schultz, 1969). Greene–Kelly's (1955) Li-test causes no decrease in expansibility in the Ticul and Tepakan samples and only a barely perceptible decrease in the Becal sample, so the layers apparently have a large amount of $Al^{3+}$-for-$Si^{4+}$ substitution.

*Exchangeable cations and capacity (CEC)*

Half-gram splits of the purified $<\frac{1}{4}\mu$ samples used for X-ray and chemical analyses were leached overnight in 75 ml of neutral $NH_4Cl$. Leachates were separated by centrifugation, the samples washed chloride-free with methanol, and the washings added to the leachate. Analysis of leachates for Ca and Mg was by Versene titration and for Na and K by flame photometry. Results (Table 2) show a reasonably good agreement between the sum of the determined exchangeable cations expressed as oxides and the amounts of CaO and $Na_2O$ reported in the chemical analyses (Table 3). About one-fourth of the Mg in each sample is exchangeable. The amounts of nonexchangeable $K_2O$ would correspond to at least 5 per cent mica or K-feldspar, amounts that would certainly be detected by X-ray. Thus, some of the layers of the mixed-layer clay must be mica-like. The CEC values indicate an increasing amount of montmorillonite from the Ticul to the Tepakan to the Becal sample, as has already been indicated by the X-ray studies (Fig. 5).

https://doi.org/10.1346/CCMN.1971.0190302 Published online by Cambridge University Press

Table 2. Exchangeable bases and cation exchange capacity (CEC) of Yucatecan clays

| me/100 g dried 110°C | Ticul $>\frac{1}{4}\mu$ | Tepakan $>\frac{1}{4}\mu$ | Becal $>\frac{1}{4}\mu$ |
|---|---|---|---|
| Ca | 34·5* | 14·9 | 25·4 |
| Mg | 13·4 | 21·3 | 25·2 |
| Na | 1·6 | 10·5 | 13·5 |
| K | nd | 3·6 | nd |
| Sum of cations | 49·5* | 50·3 | 64·1 |
| CEC | 49·5 | 52·8 | 62·8 |
| Cations expressed in per cent as oxides of chemical analyses with same $H_2O$- as on Table 3 | | | |
| CaO | 0·86 | 0·38 | 0·63 |
| MgO | 0·24 | 0·39 | 0·45 |
| $Na_2O$ | 0·05 | 0·30 | 0·37 |
| $K_2O$ | none | 0·15 | none |

*Amount given is 3·9 me less than reported, so as to correct for 0·2 per cent calcite.

[nd, not detected].

Table 3. Chemical analyses* of Yucatecan clays, in per cent

| | Ticul $<\frac{1}{4}\mu$ | Tepakan $<\frac{1}{4}\mu$ | Becal $<\frac{1}{4}\mu$ |
|---|---|---|---|
| $SiO_2$ | 43·3 | 44·5 | 45·0 |
| $Al_2O_3$ | 28·0 | 27·3 | 26·3 |
| $Fe_2O_3$ | 4·2 | 4·3 | 4·3 |
| FeO | 0·08 | 0·04 | 0·04 |
| MgO | 1·2 | 1·6 | 1·8 |
| CaO | 0·92 | 0·38 | 0·59 |
| $Na_2O$ | 0·15 | 0·47 | 0·50 |
| $K_2O$ | 0·63 | 0·96 | 0·45 |
| $TiO_2$ | 0·43 | 0·43 | 0·34 |
| Ignition loss | 21·0 | 20·0 | 20·5 |
| Sum | 100 | 100 | 100 |
| $H_2O$ to 110°C | 10·3 | 9·8 | 10·7 |
| $H_2O$, 110°–300°C | 2·9 | 2·4 | 3·1 |
| $H_2O$, 300°–1000°C | 7·8 | 7·8 | 6·7 |
| Lab. No. W- | 170690 | 170688 | 170692 |

*Rapid rock analyses, U.S. Geological Survey, Washington, D. C.

*Chemical analysis and structural formulas*

Chemical analyses of $<\frac{1}{4}\mu$ fractions of the three Yucatecan clays given on Table 3 are the basis for the calculation of structural formulas of the montmorillonite layers of the mixed-layer clay. No impurities were detected in any of the Yucatecan clays by X-ray. A trace of calcite was detected with acid under the microscope in Ticul clay. Calcite is soluble in the $NH_4Cl$ solution used to determine exchangeable cations, and from an excess in total exchangeable cations over the CEC of 3·9 me/100 g, apparently 0·2 per cent calcite was dissolved. Possible presence of amorphous material was tested by boiling splits of the three clays for 5 min in 2-per cent solutions of $Na_2CO_3$ in which amorphous alumina and silica are soluble. Resulting weight loss was less than 1 per cent in all samples, and chemical analyses of the treated clays (not given here) are essentially the same as those of untreated clay shown on Table 3; therefore the samples apparently contain no appreciable amount of amorphous material. Anatase detected in size fractions $>\frac{1}{4}\mu$ in electron micrographs (Fig. 2) and by X-ray (Table 1) suggests that the fraction of a per cent of $TiO_2$ shown for all $<\frac{1}{4}\mu$ fractions in Table 3 may also occur as anatase that is too sparse to detect by X-ray. The possible kaolinite particles shown in the electron micrographs also are too few to significantly affect the chemical composition. The main uncertainty in calculation of structural formulas from the chemical analyses lies in the assignment of proportions of kaolinite and montmorillonite within the mixed-layer clay.

Qualitatively, at least, on the basis that montmorillonite contains more $SiO_2$ and MgO, and that kaolinite contains more $Al_2O_3$ and more structural (OH) ($H_2O$, 300°–1000°C on Table 3), the chemical analyses indicate the same relative proportions of kaolinite and montmorillonite as the other data given herein, with the most kaolinite in the Ticul sample and the most montmorillonite in the Becal sample.

Structural formulae of montmorillonite layers for different kaolinite–montmorillonite proportions were calculated from the chemical analyses given on Table 3 after corrections for 0·2 per cent calcite in the Ticul sample and with the following assumptions: (1) $TiO_2$ does not occur in the clay but rather in anatase, (2) an ideal anionic framework of $[O_{20}(OH)_4]$, and (3) Mg corresponding to the determined exchangeable Mg (Table 2) occurs in interlayer positions and the remainder is in the octahedral layers of the montmorillonite. Three parameters of the montmorillonite structural formulas that should come within certain "reasonable limits" are plotted against the proportion of kaolinite on Fig. 7. "Reasonable limits" are determined as follows. Montmorillonite in the mixed-layer clays, as previously mentioned, behaves like a montmorillonite with a relatively high layer charge, i.e. about 0·85 to 1·2 or 1·3 per unit cell. Above this range the layers should behave like vermiculite when Mg–glycerol treated, which they do not. Below this range they should behave like a low-charge mont-

https://doi.org/10.1346/CCMN.1971.0190302 Published online by Cambridge University Press

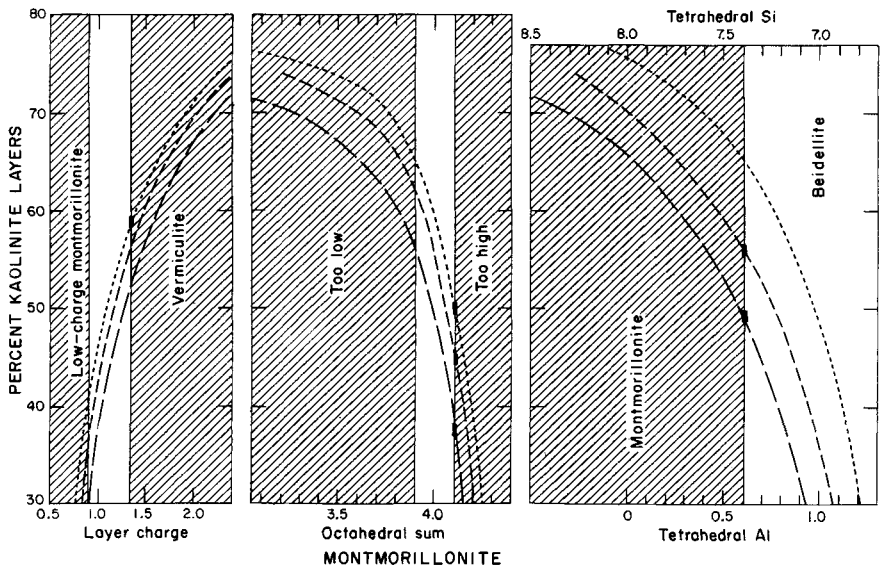



Fig. 7. Critical values of montmorillonite structural formulas calculated after subtraction of kaolinite from chemical analyses (Table 3). Areas of unreasonable values are shaded. Values limiting kaolinite to narrowest range are at heavy notches. ····· Ticul; ---- Tepakan; ——— Becal.

morillonite and re-expand fully when $K^+$–300°C–glycol treated, which they do not. The probable layer charge limits have been adjusted on Fig. 7 to slightly higher values of 0·90–1·35 per unit cell to compensate for mica layers, indicated by non-exchangeable $K^+$, which probably have a layer charge higher than average. In the center part of Fig. 7, it is considered unlikely that the sum of octahedral cations deviates by more than 0·10 from the ideal 4·00 per unit cell. On the right side of Fig. 7 the unbalanced charge in the tetrahedral sheet due to $Al^{3+}$-for-$Si^{4+}$ substitution is assumed to be at least 0·60 per unit cell, and is probably higher, in order to account for the beidellitic behavior of the montmorillonite toward Greene–Kelly's (1955) Li-test. Ticul clay is limited to 50–59 per cent kaolinite layers because above this the montmorillonite would have the layer charge of a vermiculite, and below this limit the total of octahedral cations is too high for a dioctahedral clay. Tepakan clay is limited to 45–56 per cent kaolinite layers and Becal clay is limited to 38–49 per cent kaolinite layers by the 0·60 tetrahedral Al line and the 4·10 octahedral sum line. Midpoints for these probable ranges, rounded to the nearest 5 per cent, are 55, 50, and 45 per cent kaolinite layers for Ticul, Tepakan, and Becal clays. The average composition of the montmorillonite layers calculated for the three clays after subtracting $SiO_2$ and $Al_2O_3$ for these proportions of kaolin layers is:

$$K_{0.2}Na_{0.2}Ca_{0.2}Mg_{0.2}(Al_{2.5}Fe_{1.0}Mg_{0.5})(Al_{0.7}Si_{7.3})\text{-}O_{20}(OH)_4.$$

*Differential thermal analysis (DTA)*

Differential thermal traces were made from approximately 0·5 g samples of the three Yucatecan clays packed into wells of a nickel block and with temperature increased at 10°C/min. The three DTA traces are so similar that the trace for only one sample is shown in Fig. 8. Peak temperatures and areas are given in Table 4. The slight increase in the area of the endotherm due to volatilization of interlayer and adsorbed water from the Ticul to the Becal sample is in accord with the previously inferred increase in montmorillonite through this series. A second endotherm commonly

Table 4. Peak temperatures and areas from DTA for thermal reactions of Yucatecan clays

| Reaction | | Ticul | Tepakan | Becal |
|---|---|---|---|---|
| Interlayer and | *T* | 150 | 150 | 150 |
| adsorbed $H_2O$ | *A* | 5·22 | 5·54 | 6·13 |
| Structural | *T* | 565 | 565 | 565 |
| (OH) | *A* | 13·92 | 13·01 | 12·70 |
| Ending | *T* | 890 | 895 | 900 |
| | *A* | 4·64 | 4·13 | 4·64 |

[*T*, temperature in °C; *A*, area in cm²].

https://doi.org/10.1346/CCMN.1971.0190302 Published online by Cambridge University Press

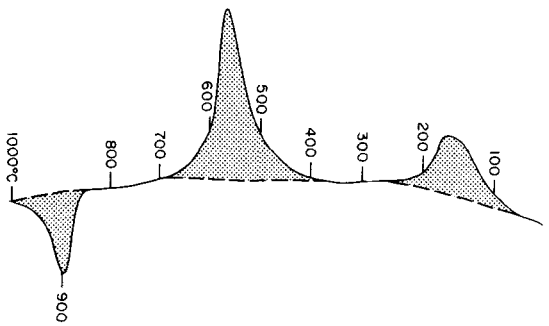



Fig. 8. DTA curve of $< \frac{1}{4}\mu$ Tepakan clay. Shading indicates area measured for peak area on Table 4.

given by double-water-layer Ca-montmorillonites is unaccountably absent. The size of the 565°C endotherm due to loss of structural (OH) increases slightly from the Becal to the Ticul sample. This increase reflects more kaolin layers in the Ticul sample inasmuch as kaolinite ideally contains about 14 per cent and montmorillonite about 4 per cent structural (OH). The DTA traces show no sign of a dehydroxylation endotherm near 700°C as is normal for montmorillonite. Thus, the montmorillonite layers are a non-ideal variety and may contain amounts of structural water different from the ideal 4 (OH) per unit cell (Schultz, 1969). When the samples are fired to 1000°C they become amorphous.

*Thermal gravimetric analysis (TGA) and structural (OH)*

A TGA curve was made only of the Tepakan sample (Fig. 9). Air was first pumped from the sample enclosure to eliminate effects of convection currents and to consolidate all buoyancy correction due to change in density of the air into this first part of the curve. At point B on the curve, the furnace

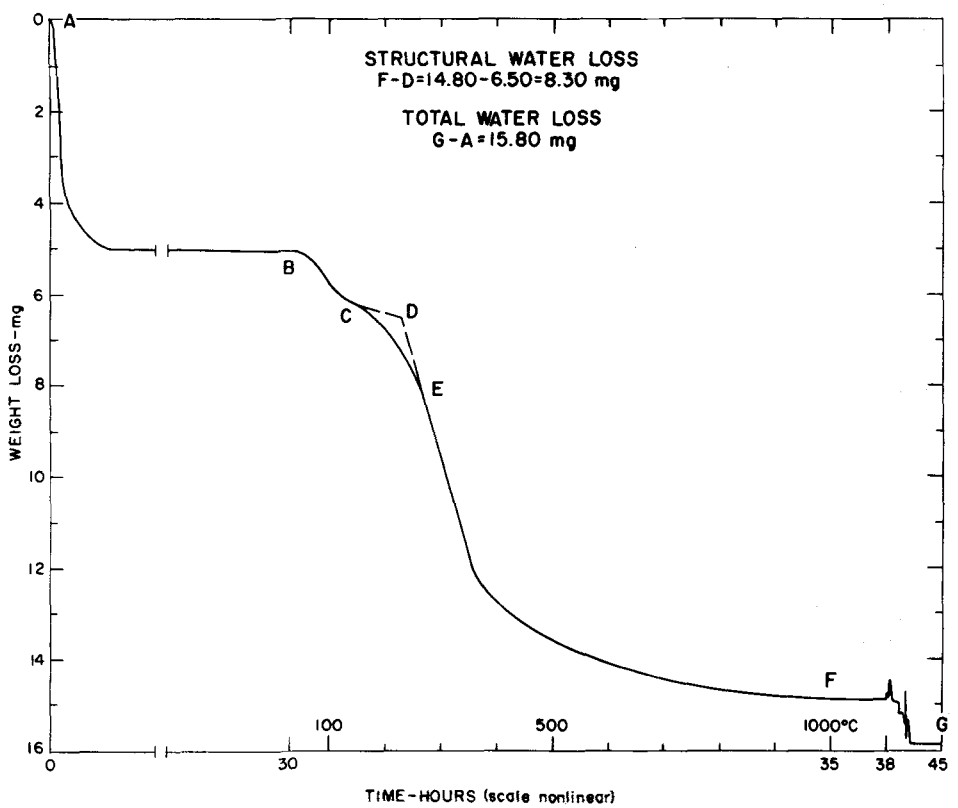



Fig. 9. TGA curve of a 100-mg sample of air-dried $< \frac{1}{4}\mu$ Tepakan clay. Vacuum applied at A and maintained at 10 mm Hg to F. Heating began at B and temperature raised at 100°C/hr to 1000°C at F where it remained for 3 hr; then temperature and pressure stabilized to room conditions at G over a 7-hr interval.

https://doi.org/10.1346/CCMN.1971.0190302 Published online by Cambridge University Press

was turned on and the temperature raised at 100°C/hr to 1000°C and maintained there for 3 hr. The balance, after some bouncing during cooling and release of the vacuum, stabilized at G at a point 1·00 mg greater than at point F, before the release of the vacuum. This 1·00 mg represents the buoyancy loss and is added to the 5·10-mg weight loss from points A to B, during vacuum pumpdown.

Point D is the intersection of straight lines drawn from inflections in the curve at C and E. On a comparative curve made under identical conditions on this same apparatus of a sample from Chambers, Arizona (Schultz, 1969, Table 4), the weight loss between similarly derived points D and F corresponded exactly to the ideal 4·00 (OH) per unit cell. As the Chambers sample is believed, in fact, to contain an ideal amount of structural water, point D is also used to evaluate what is believed to be a true structural water value for the Tepakan clay.

The 8·30-mg weight loss from points D to F on Fig. 9 is 8·30 per cent of the original 100 mg air-dried sample. The total weight loss from A to G of 15·8 per cent of the sample air dried in Denver is considerably less than the 20·0-per cent ignition loss when the sample was chemically analyzed in Washington, D.C. (Table 4). Because of different degrees of hydration, samples are compared on the basis of their ignited weight. The 8·30 per cent from TGA is 9·86 per cent of the ignited weight. The 7·8-per cent water loss between 300° and 1000°C corresponds to 9·75 per cent of the ignited weight, and is in remarkably good agreement with the TGA measurement. The 300°–1000°C water losses of the Ticul and Becal samples (Table 4) correspond to 9.88 per cent and 8·42 per cent of the ignited samples. The structural (OH) values are thus qualitatively in accord with a kaolinite–montmorillonite composition of the samples, as they are midway between the ideal values of 16·2 per cent of ignited weight for kaolinite and about 5 per cent for montmorillonites.

Amounts of structural (OH) for different kaolinite–montmorillonite ratios calculated from the TGA curve of Tepakan clay, from the 300°–1000°C weight loss of all three samples, and assuming ideal structural water in the kaolinite are shown on Fig. 10. The most reliable data, from the TGA run, indicate a slight deficiency of structural (OH) for the minimum probable proportion of kaolinite layers in the Tepakan sample indicated by the chemical data, and for the "best guess" shown by the point of the bracket the deficiency is much greater, with only about 3(OH) per unit cell. The amount of 300°–1000°C water is slightly more deficient for the Tepakan sample than is calculated from TGA, and is much more deficient for the Becal and the Ticul samples.

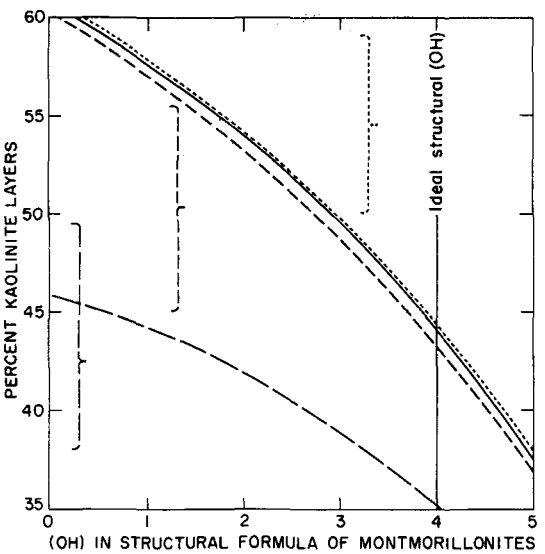



Fig. 10. Structural (OH) of three Yucatecan clays calculated from TGA and 300°–1000°C weight loss (Table 3), assuming ideal structural (OH) in kaolinite layers. Brackets indicate range of probable percentages of kaolinite layers in the mixed-layer clay judged from chemical analyses. TGA of Tepakan clay, ————; 300°–1000°C weight loss of Ticul ·····, Tepakan -----, and Becal — — clays.

Deviation of structural (OH) from an ideal of 4 per unit cell will affect the structural formulas, because the assumed negative charge of 44 per cell $[O_{20}^{2-}(OH)_4^{-1}]^{-44}$ will not be correct. Calculations evaluated as on Fig. 7, but including the amount of structural (OH) indicated by the 300–1000°C weight loss instead of the ideal 4 (OH), result in a lower and even narrower reasonable range for proportions of kaolinite layers that give reasonable structural formulas for the montmorillonite layers – about 45 per cent kaolin layers in Ticul and Tepakan and 35 per cent in Becal clay. These proportions yield an average structural formula for the montmorillonite layers of $K_{0·2}$ $Na_{0·2}$ $Ca_{0·2}$ $Mg_{0·1}$ $(Al_{2·9}$ $Fe_{0·8}$ $Mg_{0·5})$ $(Al_{0·8}$ $Si_{7·2})$ $O_{20·3}$ $(OH)_{3·7}$. The sum of the octahedral cations of 4·2 is a bit high, but if the assumed proportion of kaolin layers is reduced further the layer charge becomes unrealistically low.

The absolute numbers used in the five preceding paragraphs should be taken with caution. Structural (OH) is very difficult to determine with confidence, though the vacuum apparatus does eliminate some uncertainties inherent in the analyses performed in the atmosphere. Also, we have no way of knowing if the (OH) deficiency of the clays is in the montmorillonite or the kaolinite layers. We

https://doi.org/10.1346/CCMN.1971.0190302 Published online by Cambridge University Press

do believe that the data provide a fairly good qualitative case for some deficiency in structural (OH) in the three Yucatecan clays. The data are certainly in accord with the basic mixed-layer kaolinite–montmorillonite composition inferred from all other data for the clays, and the inferred (OH) deficiency is in accord with the absence of an ~ 700° endotherm expected for ideal montmorillonite as discussed in connection with the DTA results.

## REFERENCES


Altschuler, Z. S., Dwornik, E. J. and Kramer, H. (1963) Transformation of montmorillonite to kaolinite during weathering: *Science* **141**, 148–152.

Brindley, G. W. (1961) Experimental methods, and Kaolin, serpentine, and kindred minerals. In *X-ray Identification and Crystal Structures of Clay Minerals* (Edited by Brown, G.), pp. 1–131. The Mineralog. Soc., Clay Minerals Group, London.

Brindley, G. W. and Souza Santos, P. de (1966) New varieties of kaolin group minerals and the problem of finding a suitable nomenclature: *Proc. Internat. Clay Conf., Jerusalem*, 3–9.

Brown, G. and MacEwan, D. M. C. (1951) X-ray diffraction by structures with random interstratification. In *X-ray Identification and Crystal Structures of Clay Minerals* (Edited by Brindley, G. W.), pp. 314–320. The Mineralog. Soc., Clay Minerals Group, London.

Butterlin, J. and Bonet, F. (1963) Mapas geológicos de la península de Yucatán – I. Las formaciones cenozóicas de la parte mexicana de la península de Yucatan: *Ingeniería Hydraul. México* **17**, 63–71.

Greene-Kelly, R. (1955) Dehydration of the montmorillonite minerals: *Mineralog. Mag.* **30**, 604–615.

Klug, H. P. and Alexander, L. E. (1954) *X-ray Diffraction Procedures* 716 p. Wiley, New York.

MacEwan, D. M. C. (1961) Montmorillonite minerals. In *X-ray Identification and Crystal Structures of Clay Minerals* The Mineralog. Soc., Clay Minerals Group, London. (Edited by Brown, G.), pp. 143–207.

MacEwan, D. M. C., Ruiz Amil, A. and Brown, G. (1961) Interstratified clay minerals. In *X-ray Identification and Crystal Structures of Clay Minerals* (Edited by Brown, G.), pp. 393–445. The Mineralog. Soc., Clay Minerals Group, London.

Mooney, R. W., Keenan, A. G. and Wood, L. A. (1952) Adsorption of water vapor by montmorillonite: *J. Am. Chem. Soc.* **74**, 1367–1374.

Poncelet, G. M. and Brindley, G. W. (1967) Experimental formation of kaolinite from montmorillonite at low temperatures: *Am. Mineralogist* **52**, 1161–1173.

Ross, M. (1968) X-ray diffraction effects by non-ideal crystals of biotite, muscovite, montmorillonite, mixed-layer clays, graphite, and periclase: *Z. Kristall.* **126**, 80–97.

Ruiz Amil, A., Ramirez Garcia, A. and MacEwan, D. M. C. (1967) X-ray Diffraction Curves for the Analysis of Interstratified Structures: *Inst. Quimica Inorg.* 179.

Schultz, L. G. (1969) Lithium and potassium absorption, dehydroxylation temperature, and structural water content of aluminous smectites: *Clays and Clay Minerals* **17**, 115–149.

Shimoyama, A., Johns, W. D. and Sudo, T. (1969) Montmorillonite–kaolin clay in acid clay deposits from Japan: *Proc. Internat. Clay Conf., Tokyo* 225–231.

Sudo, T. (1959) *Mineralogical Study on Clays of Japan* 328 p. Maruzen Tokyo.

Sudo, T. and Hayashi, H. (1955) Types of mixed-layer minerals from Japan: *Clays and Clay Minerals* **4**, 389–412.

Thompson, R. H. (1958) *Modern Yucatecan Maya pottery making*. Supp. 23, 157 p. Am. Antiquity.



**Résumé** – Les couches d'argile de 1 à 2 m d'épaisseur alternant avec des calcaires marins datant probablement du début de l'éocène, sont composées d'un interstratifié kaolinite–montmorillonite à peu près pur. L'étude de la taille des particules, les micrographies électroniques, la diffraction des rayons X, les analyses chimiques, les expériences d'échange de cations, l'ATD et l'ATG, indiquent que les argiles provenant de trois localités différentes contiennent en proportion à peu près égale des feuillets de kaolinite et de montmorillonite interstratifiés au hasard. La montmorillonite a en moyenne la formule structurale $K_{0,2}Na_{0,2}Ca_{0,2}Mg_{0,2}(Al_{2,5}Fe^{3+}_{1,0}Mg_{0,5})(Al_{0,75}Si_{7,25})O_{20+}(OH)_{4-}$, avec un déficit d'OH de structure aussi bien dans les feuillets de montmorillonite que de kaolinite. Du potassium non échangeable indique que quelques feuillets sont du type mica. Les cristaux sont le plus souvent des plaques arrondies d'un diamètre allant de 1/10 à 1/20 $\mu$. Le diagnostic essentiel du caractère interstratifié est un pic de diffraction X voisin de 8 Å après chauffage à 300°C. On suppose que les argiles se sont développées par altération d'une cendre volcanique, suivie d'une érosion et d'un dépôt dans des bassins protégés voisins de la côte.



**Kurzreferat** – Tonbetten von 1–2 m Stärke und zwischengelagert mit Meerkalkstein aus dem frühen Eozän setzen sich aus fast reinem gemischtschichtigem Kaolinit–Montmorillonit zusammen. Untersuchungen der Teilchengrösse, Elektronenmikrographien, Röntgenbeugungsuntersuchungen, chemische Analysen, Kationenaustauschversuche, DTA und TGA deuten darauf hin, dass Tone von drei verschiedenen Fundorten ungefähr gleiche Anteile unregelmässig zwischengelagerter Kaolinit- und Montmorillonitschichten enthalten. Die Montmorillonitstrukturformeln umfassen im Durchschnitt $K_{0,2}Na_{0,2}Ca_{0,2}Mg_{0,2}(Al_{2,5}Fe^{3+}_{1,0}Mg_{0,5})(Al_{0,75}Si_{7,25})O_{20+}(OH)_{4-}$, mit einem Mangel an strukturellem (OH) in entweder den Montmorillonit- oder den Kaolinitschichten. Nichtaustauschbare $K^+$ zeigen an, dass einige Schichten glimmerähnlich sind. Die Kristalle sind meist runde Plättchen von 1/10 bis 1/20 $\mu$




https://doi.org/10.1346/CCMN.1971.0190302 Published online by Cambridge University Press

Quermass. Das eindeutigste Merkmal des Gemischtschichtcharakters ist eine Röntgenreflexion nahe 8 Å nach Erwärmung auf 300°C. Es wird vermutet, dass sich die Tone durch Verwitterung vulkanischer Asche und nachfolgender Erosion und Ablagerung in geschützten, küstennahen Bassins gebildet haben.

**Резюме** — Глинистые пласты мощностью 1–2 м, переслаивающиеся с морским известняком, возможно, раннеэоценового возраста, состоят из почти чистого смешанно-слойного каолинит-монтмориллонита. Изучение размеров частиц, данные электронной микроскопии, рентгенографии, химического анализа, изучение катионообменных свойств, ДТА и ТГА показали, что глинистый минерал трех различных месторождений содержит примерно равные доли беспорядочно чередующихся каолинитовых и монтмориллонитовых слоев. Усредненная структурная формула монтмориллонита:

$$K_{0,2}Na_{0,2}Ca_{0,2}Mg_{0,2}(Al_{2,5}Fe^{3+}_{1,0}Mg_{0,5})(Al_{0,75}Si_{7,25})O_{20}(OH)_{4};$$

характерен дефицит структурных гидроксилов как в монтмориллонитовых, так и в каолинитовых слоях. Наличие необменных ионов $K^+$ указывает на слюдяную природу некоторых слоев. Кристаллы в большинстве случаев представляют округлые пластинки с диаметром 1/10–1/20 мк. Наиболее вероятным диагностическим признаком смешанно- слойного характера минарала является рентгеновское отражение около 8 Å образцов, нагретых до 300°. Эти глины образовались при выветривании вулканического пепла с последующим переотложением в околобереговых бассейнах.

https://doi.org/10.1346/CCMN.1971.0190302 Published online by Cambridge University Press